

RESEARCH ARTICLE OPEN ACCESS*Soil Health: Current Status and Future Challenges*

Printed PHBV-Based Sensors as a Real-Time Proxy for Soil Microbial Decomposer Activity During Drought and Flood Recovery

Ellen L. Fry^{1,2} | Taylor J. Sharpe³ | Madhur Atreya³ | Gregory L. Whiting³ | John N. Quinton² ¹Department of Earth and Environmental Sciences, The University of Manchester, Manchester, UK | ²Lancaster Environment Centre, Lancaster University, Lancaster, UK | ³Paul M Rady Department of Mechanical Engineering, University of Colorado Boulder, Boulder, Colorado, USA**Correspondence:** John N. Quinton (j.quinton@lancaster.ac.uk)**Received:** 19 December 2025 | **Revised:** 5 May 2026 | **Accepted:** 20 May 2026**Keywords:** decomposition | dynamic monitoring | low-cost sensing | microbial activity | printed electronics | sensors

ABSTRACT

Improving accuracy of soil decomposition measurements for assessing carbon storage requires high spatial and temporal resolution. To advance the field, continuous, in situ, non-destructive methods of assessing microbial activity are essential. Here we demonstrate a method to track soil biological activity in real time, by monitoring the change in resistance of sensors based on a biodegradable composite material as it is decomposed by soil microbial activity. These sensors are fabricated using printing techniques and provide a straightforward resistive readout, enabling their interrogation with simple low-cost electronic systems, thereby providing a path to wide-scale deployment to provide spatial and temporal characterization of soil biological activity. Using these sensors, microbially derived decomposition of the sensors was monitored in mesocosms comparing species rich grassland soil and a monoculture wheat soil, subjected to either a drought or flooding treatment with a subsequent recovery period. The sensors tracked their decomposition every 30 min for 7 weeks, with decomposition activity subdued by the drought and demonstrate recovery following its cessation. Flooding produced a similar response in the species rich grassland, albeit the recovery was slower. However, in wheat soil, flooding did not reduce decomposition of the sensor which we attribute to wheat maintaining an oxygenated rhizosphere. The developed sensors can shed light on the dynamic nature of soil microbial processes that would otherwise go unobserved.

1 | Introduction

The role that healthy soils play in supporting ecosystem function and food production has received increasing attention in recent years. The need to understand changes in soil health has resulted in several indicators being developed for soil health assessment, which commonly include parameters relating to soil carbon (Lehmann et al. 2020). Carbon-based molecules form the basis of soil organic matter, which is a key variable in governing nutrient release, water holding capacity and soil fertility (Hoffland et al. 2020), and is central to the assessment of soil health (Bagnall et al. 2023). While soil organic matter is formed

and lost through numerous abiotic and biotic factors, it is the decomposition, specifically by microbes, that is of key importance. However, monitoring this process in real time has proved elusive.

Typically, indicators of soil health, whether soil chemical, physical or biological parameters, are determined at one point in time, either in the field or in the laboratory. Many indicators vary spatially and temporally, yet, except for a few physical and chemical parameters, e.g., soil moisture content and electrical conductivity, temporal resolution is limited to the time-point when the samples were taken. Measurements of enzymatic activity, soil nutrient concentrations and soil texture require destructive soil

This is an open access article under the terms of the [Creative Commons Attribution](https://creativecommons.org/licenses/by/4.0/) License, which permits use, distribution and reproduction in any medium, provided the original work is properly cited.

© 2026 The Author(s). *European Journal of Soil Science* published by John Wiley & Sons Ltd on behalf of British Society of Soil Science.

Highlights

- In situ, non-destructive methods are needed to track decomposition in soil through time.
- We present novel sensors that can be deployed in multiple locations and made cheaply.
- We show decomposition of the sensors in contrasting soil types under water stress at high temporal resolution.
- In situ sensors can track soil decomposition activity more effectively than traditional lab methods.

collection that disturbs and destroys the soil being monitored. Options for monitoring the temporal changes in soil biological activity are extremely limited.

Field methods for determining soil biological activity focus on the central role of decomposition of organic matter by microbes. The need for a standardised approach to measuring decomposition rates is well recognised: it must provide robust results that respond to changes in soil conditions resulting from soil management practices or wider environmental changes, and must not disturb the soil, as this artificially increases microbial decomposer activity (Hayes et al. 2024; Keuskamp et al. 2013; Middleton et al. 2021). Nevertheless, to date it has been difficult to produce dynamic data since the available methods depend upon slow mass losses. Therefore, determining how decomposition rates fluctuate in response to changes in the soil environment which take place over time periods of hours or days is difficult. Scientists have relied on the use of CO₂ gas emissions from soil surfaces to generate proxy data with increased temporal resolution. High temporal resolution can be achieved through a regular sampling system, but considerable investment in field analytical equipment is required with typical deployments restricted to arrays of 6–12 sampling points (Harmon et al. 1999). Recent research has demonstrated the use of low-cost NDIR CO₂ sensors for ex situ (Irving et al. 2024) or in situ (Joshi Gyawali et al. 2019; Macagga et al. 2024; Zeng et al. 2026) experiments, with flux measurements correlated to more expensive field equipment, showing progress towards more scalable and affordable solutions. However, these systems are largely bespoke designs that lack optimised readout electronics, telemetry, power, and enclosure solutions and have not yet entered wide-scale production or use. Furthermore, CO₂ flux at the soil surface comprises heterotrophic and autotrophic respiration by both microbes and plant roots, representing the net response of soil organisms and plants to changing environmental conditions (Ryan and Law 2005) and is not solely a measure of soil organism activity. Disentangling the respective contributions of plants and microbes to CO₂ emissions is difficult, especially under changing conditions. Given that CO₂ fluxes from soils are known to vary spatially, in response to changing soil properties, management and vegetation (Regina and Alakukku 2010), and that emissions are also temporally variable, changing diurnally, seasonally and in response to meteorological and disturbance events (Anthony and Silver 2021), current techniques have serious limitations for quantifying soil biological activity, and new approaches that directly measure microbial decomposition processes in soil are required.

To meet the need for in situ, highly temporally resolved measurements of microbially driven decomposition, our team has developed a decomposition sensor based on low-cost printed electronics (Atreya et al. 2023). Our previous work has demonstrated that we are able to translate microbial decomposition activity into a change in electrical resistance as a poly(hydroxybutyrate-co-valerate) (PHBV)/carbon composite conductor is degraded (Atreya et al. 2023). The PHBV biopolymer, which can degrade in both aerobic and anaerobic conditions, is blended with carbon flake to form a printable ink. The ink is screen-printed onto a surface, creating a resistor that is responsive to microbial activity. As microbial activity degrades the polymer, in the presence of soil moisture, it swells. This drives the carbon particles apart and increases the resistance over time, with the rate of change in resistance reflecting microbial activity. PHBV has similar characteristics to naturally occurring organic matter produced by bacteria from sugars and lipids, is used as an energy store by many bacteria, and it has come into widespread use as a biodegradable plastic. In laboratory incubations in soil PHBV has been shown to be decomposed by a wide range of bacteria and fungi; further, the degradation of polyhydroxybutyrates has been shown to be related to the functional diversity of soil microorganisms (Dey and Tribedi 2018). Thus, the sensors provide a method by which the degradation activity of microbial communities in soil can be more directly measured. In interference experiments (Atreya et al. 2023; Sharpe et al. 2026), changes in soil temperature, moisture, and salinity produce temporary and reversible changes in sensor resistance, where experiments in live soils and biologically active aqueous solutions permanently increase sensor resistance. Additionally, identical sensors made with non-biodegradable binders show no discernible response in biologically active media, and conversely, PHBV-based sensors in sterile media show no discernible response. Applications of the sensor, thus far, have focused on laboratory evaluations demonstrating proof of concept (Atreya et al. 2023), and a more extensive field application (Sharpe et al. 2026). The latter, where 44 sensors were deployed for 50 days in a long-term grassland restoration experiment in the UK, demonstrated a positive relationship between sensor response and microbial biomass carbon. Here, we expand on this work by deploying improved sensing hardware and exploring whether the sensors can capture dynamic shifts in sensor decomposition rates in response to changes in environmental stresses, such as soil moisture status. In this work, we (i) test the ability of the sensors to track the response of microbial activity to the environmental stress, and its alleviation, associated with floods and droughts in two contrasting soil and vegetation settings and (ii) compare the information provided by the sensors with traditional methods of assessing microbially mediated activity as a proxy for soil decomposition, including enzymatic activity, soil respiration and soil nutrient concentrations.

2 | Materials and Methods

2.1 | Experimental Setup

Intact cores were collected from two sites near Penrith, north-west England with the same soil type: a sandy loam of the Newport Series (Dystric Arenosol). The first was planted with

a monoculture of Winter Wheat (WW) (*Triticum aestivum* L.) (54°45'17" N, 2°47'28" W). The second was a species rich grassland (SRG) (54°43'23" N, 2°43'33" W), which had not been subjected to any chemical inputs in living memory and, given the plant biodiversity, has probably never received fertiliser inputs. The species mix included *Carex flacca*, *Plantago lanceolata*, *Lolium perenne*, *Lotus corniculatus* and *Anthoxanthum odoratum*. The cores were collected by inserting sections of pipe into the soil and removing the intact core, to reduce disturbance to the soil. The sections were 15 cm deep with a 10 cm diameter. Eighteen cores were collected from each site on 26th March and a further 18 on 10th April 2024 and placed in a polytunnel at the Hazelrigg Research Station at Lancaster University (54°0'52" N, 2°46'40" W). Each pot was assigned a random number, and one of three treatments: drought, flood, or control. The final experimental design was 2 vegetation types × 3 climate treatments × 6 replicates = 36 cores. The climate treatment began on 11th April, and it continued for 32 days, with recovery beginning on the 13th May. For the flood treatment, cores were placed in a tank with rainwater collected from the site, maintained level with the top of the soil throughout the study. For the control, watering with rainwater was administered three times a week, as needed. The drought cores were left to dry down through the treatment phase. When the treatments were alleviated, the flooded cores were allowed to drain, and the drought treatment received 1 L of fresh rainwater per pot. For the recovery period, all cores received 500 mL twice per week and were allowed to drain freely. Cores were harvested on the 18th June after 36 days of recovery.

2.2 | Decomposition Sensors

Sensors were fabricated through a hybrid printing process comprising a 3D-printed deployment carriage, a conventionally-manufactured printed circuit board (PCB), and stencil-printed ink traces composed of a mixture of PHBV and carbon flake. The experimental setup and specific geometries of the sensors deployed are shown in S1. We have described the use of this material as a decomposition sensor in a previous publication (Atreya et al. 2023). Suspended carbon flake makes the ink conductive, and as the PHBV matrix is degraded by soil microbes, the conductivity of the ink changes and can be read as a resistance change by low-cost electronics.

Where in previous work we used glass slides as the printing substrate, in this new design, the ink was printed directly onto exposed pads on the PCB in a set of three conductive strips, using transfer tape and a razor blade. Each strip was printed in a dog-bone geometry with a primary trace width of 1 mm and a length of 25 mm. All conductive strips on a single PCB were electrically connected in parallel, a configuration that controls for stochastic variability or mechanical damage impacting a single trace. Following ink printing, signal conductors were soldered to the PCB before installation in the deployment carriage. A transport and installation carriage was 3D-printed on a consumer FDM machine (i3MK3, Prusa Research) using a non-dyed PLA filament (Hatchbox). The carriage serves to protect the PCB and ink traces from mechanical damage during installation and provides a potting dam to encapsulate electrical connections. A weatherizing adhesive (FlexSeal) was poured into the potting dam and allowed to cure for at least 48 h. Between fabrication and deployment, the ink traces were protected using a 3D-printed travel sheath (Figure 1).

Sensors were deployed in each sample pot using a 3D-printed nylon installation spade in the case of all treatments except the drought cores. The installation spade creates a pre-formed cavity into which the sensor is press-fit to encourage good surface contact with the surrounding soil. In the case of the drought cores, the soil was too dry for this installation method. Instead, soil was manually excavated to form a cavity large enough for the sensor to be installed, then packed back down around the sensor. During each sensor's installation, its resistance was monitored during insertion to ensure that the traces were not mechanically damaged prior to the experiment. Initial resistances immediately following insertion, as well as normalized resistances at the start of the first decomposition window, are shown in Figure S1.

Sensor resistances were collected using custom data loggers which use the voltage-divider principle to calculate the resistances of sensors installed across six channels per logger. Resistance readings were gathered every 30 min and logged to an SD card. In this experiment, one channel from each logger was used to monitor each treatment to avoid any systematic error introduced by logger electronics and to prevent data loss if a logger were to fail mid-experiment.

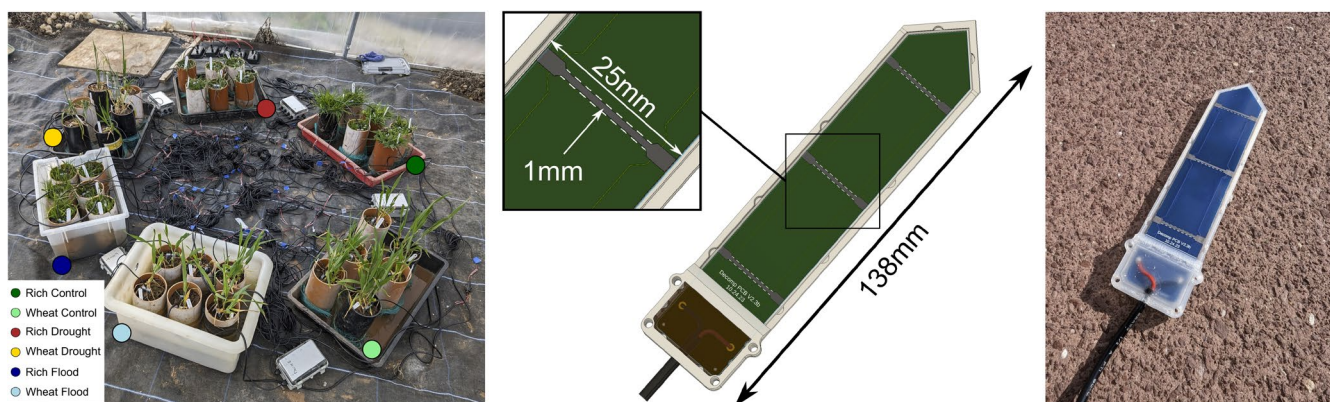


FIGURE 1 | Six replicates of six soil type and treatment combinations (left) were implemented with decomposition sensors comprising a biodegradable ink printed on a printed circuit board substrate (centre). The sensing surface is assembled within a 3D-printed deployment carriage which facilitates installation in soil and protects electrical connections with an epoxy dam (right).

2.3 | Soil Respiration and Covariates

Soil moisture and temperature were measured twice per week throughout the treatment and recovery time using an HH2 Moisture Meter with attached WET-2 sensor (Delta-T Devices, Cambridge, UK). Soil respiration was measured weekly using an EGM-5 infra-red gas analyser (IRGA) with attached SRC-2 soil respiration sensor (Hansatech, King's Lynn, UK). The chamber was modified using a piece of pipe 15 cm long to extend the chamber's height and prevent crushing of vegetation. Data were collected in the form of $\text{mg CO}_2 \text{ m}^{-2} \text{ h}^{-1}$. Air temperature was measured using an onboard sensor in the data loggers.

2.4 | Plant Analyses

Aboveground biomass was collected by cutting all vegetation at the soil surface in each core. The biomass was placed in paper bags and dried at 105°C for 48 h before accurately weighing. The root biomass was carefully shaken free of the soil and washed to remove all stones and soil particles. Roots were dried and weighed as for the aboveground portion.

2.5 | Soil Analyses

The soil was collected and sieved through a 2 mm sieve to remove stones and other debris, then stored at 5°C until analysis. Gravimetric soil moisture was measured by drying 5 g of fresh soil at 105°C for 24 h and calculating the proportion of water lost. For the microbial biomass carbon and nitrogen, the chloroform-fumigation method was used (Brookes et al. 1985). Briefly, 5 g of soil from each core was weighed into a glass vial, and 5 g into a 50 mL Falcon tube. The glass vials were added to a desiccator with a beaker containing 50 mL of chloroform, and a vacuum was applied. The sealed desiccator was left for 24 h to lyse all microbial cells in the soil samples. At the end of this period, the soil was added to 50 mL Falcon tubes and both fumigated and unfumigated samples were extracted for carbon and nitrogen using 25 mL 0.5 M K_2SO_4 per sample. These were shaken thoroughly on an orbital shaker for 30 min at 150 rpm. Samples were then filtered through Whatman 42 filter papers and analysed for microbial biomass carbon (MBC) using a Shimadzu TOC analyser (Shimadzu), and for microbial biomass nitrogen (MBN) using an autoanalyser (AA3, Seal Analytical, UK). The final values were calculated by adjusting for soil moisture, then subtracting the unfumigated from the fumigated portion, and finally adjusting by K_{EC} factor for carbon, and K_{EN} for nitrogen, to account for extraction efficiency (Joergensen 1996). The dried fraction of soil was ground in a ball mill and analysed for total carbon and nitrogen using an elemental combustion analyser (Elementar Vario EL, Hanau, Germany).

Soil extracellular enzymes were assayed using the methods of Jackson et al. (2013) with modifications outlined in Broadbent et al. (2022), which added artificial *p*-nitrophenyl (pNP) linked substrates to induce a colour reaction through *p*-nitrophenyl production. The enzymes assayed using this

approach were cellobiohydrolase (CBH), β -glucosidase (GLC), N-acetylglucosaminidase (NAG), β -xylosidase (XYL), and acid phosphatase (PHO). CBH and GLC are key enzymes for decomposing cellulose into glucose for microbial uptake. NAG is a step in chitin decomposition, making carbon and nitrogen available for microbes. XYL is part of the decomposition pathway for lignocellulose, and PHO breaks down organic phosphate forms into inorganic forms. Further assays were completed to measure phenol oxidase (POX) and peroxidase (PER), which are instrumental in breaking down complex polyphenols such as lignin and tannins.

2.6 | Statistical Analysis

All data analysis was carried out with R version 4.3.2 (R Core Team 2025). To remove spurious readings, a simple filter was applied to remove any resistance readings above $10 \text{ k}\Omega$ prior to any other data processing. To account for differing initial sensor resistances due to the manufacturing process, all sensor signals were normalized: an initial resistance (R_0) was calculated on a per-sensor basis by taking an average of readings within an initial-resistance time window following settling in the soil. A soil settling period began after installation on April 27th at midnight. Next, R_0 was calculated as the sensor-specific resistance between April 28th at midnight and 12 h later. Each following instantaneous resistance reading was divided by this initial resistance, yielding a normalized resistance (R_{norm}) which was taken to be the primary decomposition sensor signal, as in previous research (Atreya et al. 2022, 2023). Sensor response was characterized by taking sensor slopes for all individual sensors within each treatment window. Sensor slopes are taken to be the linear coefficient of a second-order polynomial model fit to the response of each individual sensor.

Most data analysis and visualizations are represented as treatment-specific R_{norm} averages taken at a 24-h frequency to remove diurnal effects. Sensor standard deviations within each treatment type are shown using error clouds to represent individual sensor variability within each treatment. For all analyses regarding treatment windows, the Treatment Window was taken to be all readings between May 1st and May 13th. A 3-day lag was introduced between physical intervention and the Recovery Window, which was taken to be all readings between May 16th and June 17th.

To assess the impact of initial watering treatment on soil samples following a return to control conditions, the soil characteristics at harvest were evaluated using two-way ANOVA with soil type and watering treatment as interacting main effects.

Time series data for soil moisture, temperature, and CO_2 efflux were collected through the course of the experiment (12 sampling dates for VWC and temperature, six sampling dates for CO_2 efflux). We carried out linear mixed effects models on each of these responses in turn in the *nlme* package in R (Pinheiro et al. 2023; Pinheiro and Bates 2000) using pot identity as a random factor, and sampling date, soil type and watering treatments as fixed factors with all interactions included. Response data (SMC, temperature and CO_2 efflux)

were transformed to meet the assumptions of the model where necessary. These models were not simplified. In Section 3, we represent these measurements in terms of mean value by treatment type, and show the standard error of the readings as error bars.

3 | Results

3.1 | Decomposition Sensor Response to Floods and Droughts

The rate of change of resistance, as a proxy for microbial activity, showed contrasts according to watering treatments over time (Figures 2a,b and S2). In the control treatments, where watering was consistent throughout, the sensor slope did not change significantly between the treatment and recovery periods. This was true of both the SRG and WW, although SRG cores became more variable over time (Figure 2c).

Sensor decomposition increased sharply with the alleviation of the drought treatment through rewetting in both the SRG and WW cores (Figure 2a,b) with the rate of increase in normalised resistance significantly higher (Figure 2c) in both treatments.

When the flood was removed and the cores allowed to drain, the recovery in the SRG cores was clear as expected, but at a significantly slower rate (Figure 2c) than the recovery from drought (Figure 2a,b). The flooded WW cores behaved differently. Here the flooding did not slow the rates of sensor decomposition as it had in the SRG cores, with no significant difference found between the treatment and recovery window. In all, apart from the

WW control treatment, variation between replicates increased after the recovery period started, reaching a maximum after 30 days.

3.2 | Changes in Soil Characteristics Following Droughts and Floods

Comparing the WW and the SRG soils, pH and activity of the carbon degrading enzymes CBH and GLC were all significantly higher in the WW Soil (Figure 3a,i,l and Table S1), and BGB, soil carbon, soil nitrogen and POX were significantly lower (Figure 3d-f,k and Table S1). Significant effects of the watering treatment were observed in both above and belowground biomass, where the drought and flooding both resulted in lower biomass than the control (Figure 3c,d and Table S1). Further, belowground biomass showed an interactive effect between the soil type and the watering treatment, indicating that in WW soils, drought and flooding had similar effects, while in SRG soils, drought had a more negative effect than flooding. For the soil enzymes, we observed watering effects on PER and POX, both degraders of complex carbon-based molecules, which both increased in the flooding treatment (Figure 3k,o). NAG, which degrades nitrogen-based molecules, also increased in the flooding treatment (Figure 3n). GLC, which degrades cellulose-based molecules to glucose, showed an interaction between soil type and watering treatment, where GLC was higher in WW than SRG, but while drought decreased GLC in WW, it increased in SRG (Figure 3l). Non-significant effects of the watering treatments were observed in soil carbon and nitrogen, and microbial biomass carbon and nitrogen, indicating either successful recovery or no effect of the treatments (Figure 3e-h and Table S1).

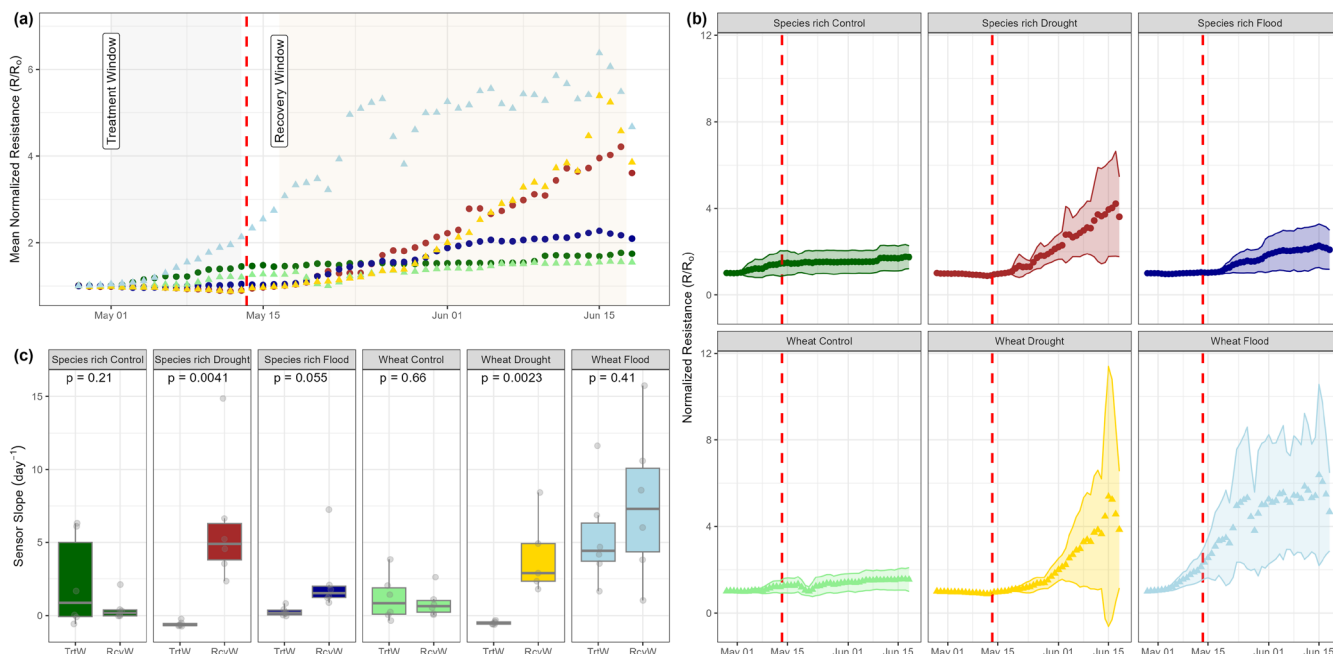
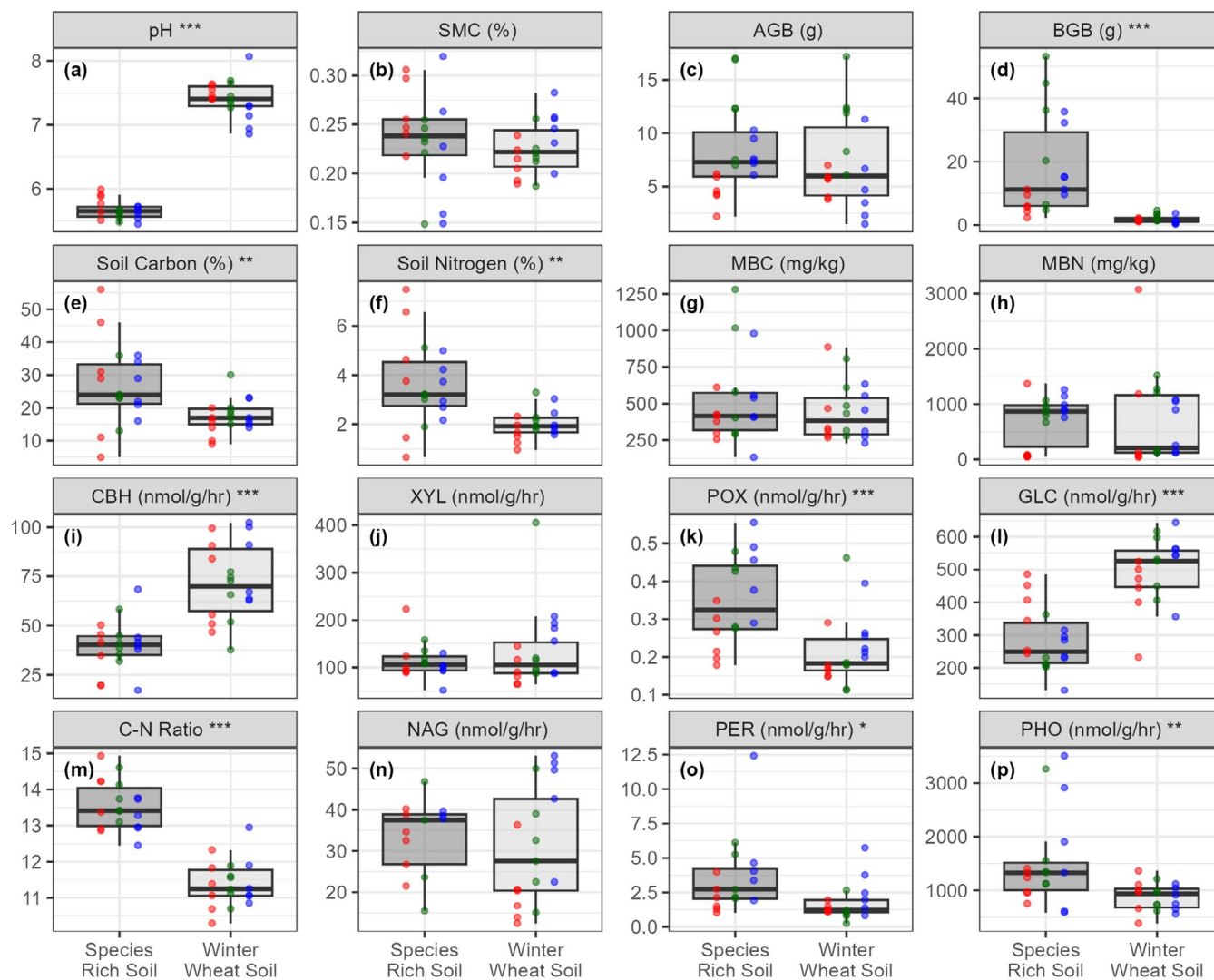


FIGURE 2 | Sensor responses were characterized in two sensor decomposition windows: While treatment effects were applied, and during recovery. (a) Normalized resistance means are shown across the sensor fleet, where visual examination reveals sensor signal changes following the removal of drought and flooding conditions. (b) Gives the standard deviation of the sensor readings and where we see a strong response between treatment and recovery windows for most treatments. (c) Within the treatment and recovery windows, we examined sensor slope distribution, illustrating the median with interquartile range (IQR, whiskers represent smallest or largest value within $1.5 \times \text{IQR}$).



Initial Treatment: ● Drought ● Control ● Flood

FIGURE 3 | Laboratory measurements were taken at the end of the experiment to characterize differences between the two soil types and to examine the recovery of cores which had been subjected to flood or drought conditions. Box plots represent the median and IQR, whiskers represent the smallest or largest value within $1.5 \times \text{IQR}$. Significance stars reflect comparisons between the two soil types, * $p < 0.05$, ** $p < 0.01$, *** $p < 0.001$. For two-way ANOVA output, see Table S1. (a) pH, (b) SMC, (c) AGB, (d) BGB, (e) soil carbon, (f) soil nitrogen, (g) MBC, (h) MBN, (i) CBH, (j) XYL, (k) POX, (l) GLC, (m) C-N ratio, (n) NAG, (o) PER and (p) PHO.

3.3 | Changes in Environmental Parameters Throughout the Experiment

Soil volumetric moisture content (Figure 4a) showed clear differences during the treatment period with the treatments converging during the recovery period. The measured CO_2 flux (Figure 4c) showed no treatment-specific response in the recovery period, with respiration in each of the treatments remaining similar throughout the experiment. No relationship was found between the measured CO_2 flux and the decomposition sensor slope (Figure S3). No clear signal was visible between treatment and control conditions when evaluated purely on CO_2 accumulation slope or integral (Figure S4). As expected, soil temperatures (Figure 4b) were on average higher during the drought treatment (average 29.5°C) than during the flooding treatment

(average 24.3°C), with the control treatment temperature between the flood and drought treatments (27.3°C on average). Average air temperature captured by the loggers (Figure 4d) showed a strong diurnal pattern with temperatures reaching a daily mean maximum of 37.3°C and a daily mean minimum of 10.7°C .

4 | Discussion

By deploying sensors in contrasting soil and vegetation settings which have been exposed to either a period of drought or waterlogging, we demonstrate in real time how the sensor decomposition rate changes following the removal of that stress. The data captures nuanced information on changes in microbial

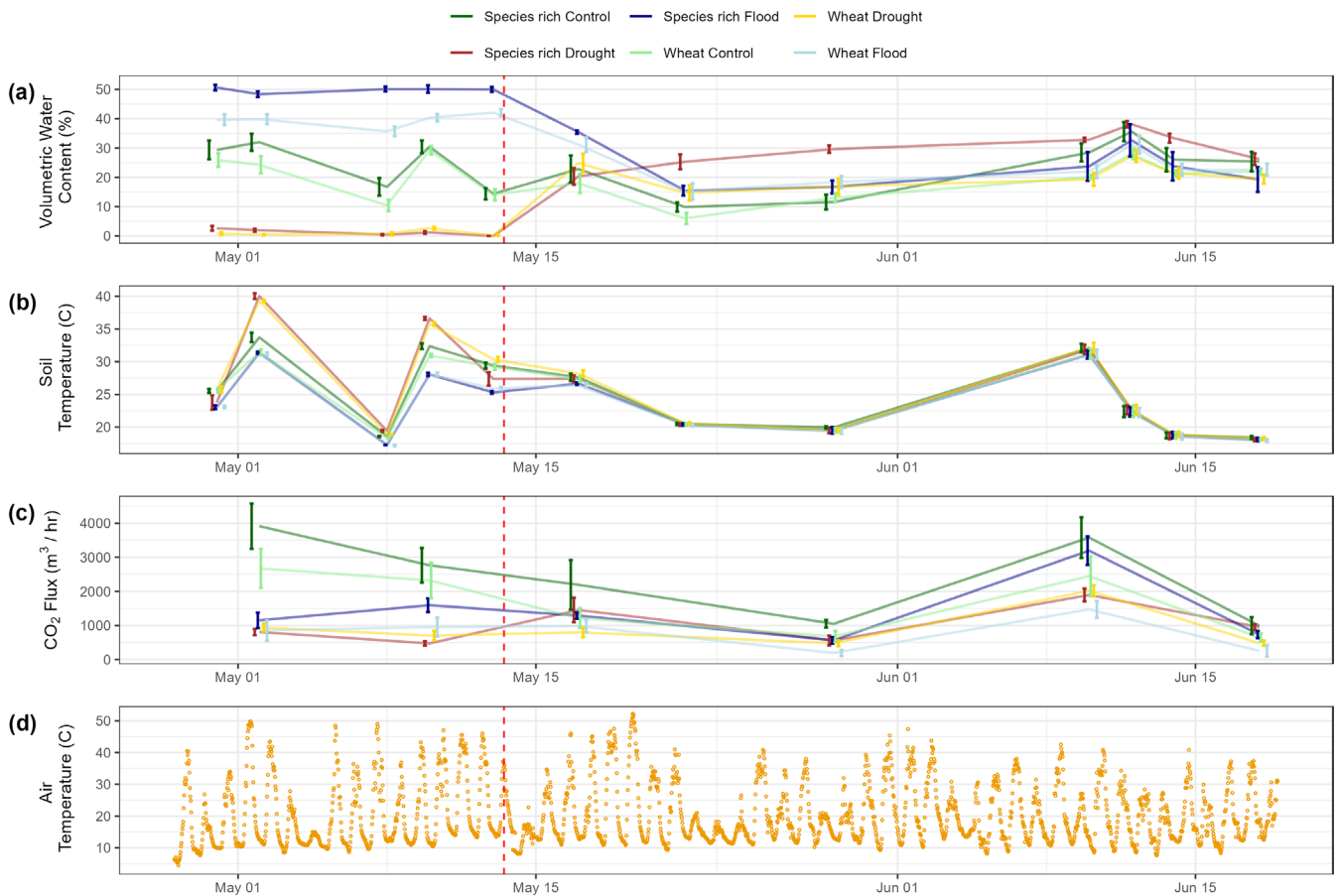


FIGURE 4 | Environmental parameters were measured throughout the experiment. Air temperature was collected by on-board sensors in the data loggers. Note that subplots (a–c) include lines only to show trends over time, not to imply continuous measurements. Error bars are standard errors of the mean. (a) Volumetric water content, (b) soil temperature, (c) CO₂ flux and (d) air temperature.

conditions in the soil in a non-destructive manner. As shown by our soil chemistry data, gathering data destructively at the end of a period of stress and recovery leaves knowledge gaps on the exact impacts of the stress on microbially-driven activity through the stress. A recovery period can obfuscate the overall decomposition rate of soil organic matter by showing apparently similar values in one snapshot of time.

After the alleviation of the drought our soil decomposition sensors responded with a rapid and strong positive shift in resistance, indicating an increased decomposition rate of the sensor substrate following alleviation of environmental stress, with both the SRG and WW treatments showing a similar rate of sensor decomposition throughout the experiment. These responses follow the expected pattern as it is well known that microbial activity sharply increases when osmotic stress is removed (Birch 1958). The main reasons for this are thought to be associated with the release of metabolites due to cell lysis upon rewetting of the soil, which then provide easily decomposable food sources for surviving organisms and the release to protected organic matter (Singh et al. 2023). However, it is acknowledged that in the case of the drought treatment, soil had to be repacked around the sensor and this may have affected the contact between the soil and the sensor, which may have influenced the result.

In the case of flooding, the picture is more complicated. In line with published work, it was expected that flooding

would cause significant impacts on soil functioning (Huang et al. 2023; Sánchez-Rodríguez et al. 2019; Tate III 1979). We expected sensor rates in the flooded cores to be lower than the control, due to anaerobic conditions being established at the sensor, thus slowing or stopping the decomposition activity of aerobic and facultative organisms and that there would be steady recovery following the cores being allowed to drain under gravity but that the recovery would be slower than in the droughted treatments. We hypothesise that this is due to the slower rate of change in soil moisture following the alleviation of flooding compared to the alleviation of the drought; this is because it takes longer for water to drain from a soil than it takes for a soil to rewet under experimental conditions. This pattern is what we observed in the SRG treatment. In contrast, in the WW the flooding had no negative impact on sensor decomposition rates; in fact, sensor decomposition rates were higher throughout the experiment in this treatment combination than in any other treatment including the controls. Further, while roots were decreased in biomass, we saw increased enzymatic activity in flooded soils. We suggest that this was potentially due to the actively growing wheat plants maintaining an oxygenated rhizosphere which promoted biological activity and thus, sensor decomposition. This may have been due to greater rates of evapotranspiration from the flooded wheat pots, possibly enhanced by the wheat plant's ability to form aerenchyma cells in their roots in response to waterlogging, which has been documented

elsewhere (Yamauchi et al. 2013). Stress may have been lower in wheat soils due to the lower moisture content in the flooded WW than in the flooded SRG (Figure 4). More work is needed to understand the interactions between the wheat roots, their response to flooding and their interaction with the soil microbial community, and future experiments should include the dynamic measurement of soil water potential and content and include plant physiology imaging, including examining roots for the presence of aerenchyma.

The soil analysis we conducted at the end of the experiments was able to show differences between the SRG and the WW cores, and we observed some effects of the watering treatments, mainly on the biomass of the plants, and the extracellular enzymatic assays, which are responsive to rapid changes in conditions. The soil measures which would be slower to respond to changes, i.e., total soil carbon and nitrogen and microbial biomass, only showed differences between soil type, as expected. The higher soil carbon and nitrogen contents in the grassland soil are in line with expectations as the regular disturbance of the arable soil increased aeration and availability of organic carbon for decomposition, and there are lower returns of plant material due to crop harvests. The higher nitrogen content in the grassland soil is perhaps a little surprising, given that the arable soil had regularly received inorganic and organic sources of fertiliser, however, offtake by the crop and leaching is likely to be higher in the arable soil than in the SRG which is essentially a closed system. Activity of hydrolase enzymes (CBH) was higher in WW cores, which is in line with other work that shows hydrolases target the labile C forms prevalent in agricultural soils and could potentially align with the sensor data. Further, activity is lower in soils with a high carbon to nitrogen ratio, as in the SRG soils. By contrast, oxidases (PER, POX), which were higher in the SRG cores than the WW in our study, target more recalcitrant carbon (Sinsabaugh 2010). SRG contains species which are more conservative in their growth form than arable crops, with slower growth leading to more complex carbon-based structures. Therefore, it is unsurprising that oxidase activity is higher in SRG cores than WW, where crop breeding has served to optimise rapid growth and low investment in roots and long-term structures in favour of high yields of reproductive organs (Poffenbarger et al. 2023). The increase in some enzyme activity in flooded soils, particularly in the wheat cores, was surprising but links with the findings of the sensors. However, the sensors were able to provide a far more nuanced dataset showing effects of the watering in real time, while the soil measures were taken destructively, some weeks after the watering treatments were alleviated. Therefore, while there is value in soil measures, the real-time non-destructive measurements provided by sensors allow for timely interventions where needed.

We were surprised to note that weekly CO₂ flux measurements were unable to detect strong consistent effects of the watering treatment. Although the lack of alignment between CO₂ fluxes and sensor slopes is perhaps to be expected, as they measure different things. Ecosystem level respiration has long been used as a simple, rapid, non-destructive proxy for ecosystem function, i.e., plant and microbial activity. However, about 50% of the measure is from heterotrophic respiration from plant roots

and mycorrhizae (Ryan and Law 2005), while the sensors are measuring a direct breakdown of the PHBV by microbial action. IRGA-based gas fluxes are also influenced by temporal fluctuations, air temperature and plant composition, which could be less important for soil sensors embedded below the soil surface (Clarkson et al. 2024). Nevertheless, we expected to see some level of correlation through the growing season and in response to the treatments, as plant and microbial activity respond to the same drivers and are intrinsically linked. This study indicates that proxy measurements may be insufficient to identify a signal from microbial activity alone.

Building from this work, there are various potential avenues for future development and understanding of these novel soil sensing devices that are currently being investigated. One interesting line of inquiry is to explore the use of other degradable materials in addition to PHBV, potentially enabling a variety of specific microbial or enzymatic processes to be selectively monitored. Additionally, carrying out genetic analysis of the microbe-sensitive composite resistor surfaces and surrounding soil to determine the composition of the microbial community responsible for changes in the recorded signal would be beneficial to enhance understanding of the function of the sensors, and to improve the interpretation of the data that they provide. Further long-term field evaluation of the sensors will aid in better understanding the impact of soil management amendments on the sensor signal and the response of the soil microbial community.

5 | Conclusions

We have shown that the sensors can provide dynamic, high temporal and spatial resolution data relating to soil microbial decomposition of the sensors. Following the alleviation of drought in both a WW and SRG soil and flooding in the SRG, their response indicates a rapid increase in microbial activity, tracked by the sensors. Additionally, the sensors have also produced results which provoke the need for further work in understanding how WW responds to flooding and may alter the rhizosphere environment.

Our study demonstrates that low-cost printable electronic sensors can autonomously track decomposition activity at high temporal and spatial resolution and offers the potential to explore the dynamics of microbial activity in soils. This has, until now, not been possible without repeated sampling of the target system. Thus, we offer the prospect of a means to study soil microbial community activity fluctuations in situ and without disturbance, beyond inserting the sensor. The low cost and small footprint of this sensor platform offer the opportunity to deploy large numbers of sensors across soil types and treatments, allowing us to elucidate the spatial response of decomposition processes to environmental and management changes.

Author Contributions

Ellen L. Fry: writing – original draft, methodology, writing – review and editing, formal analysis, data curation, conceptualization. **Taylor J. Sharpe:** investigation, writing – original draft, writing – review and

editing, visualization, formal analysis, data curation. **Madhur Atreya:** writing – review and editing, resources, methodology. **Gregory L. Whiting:** methodology, writing – review and editing, resources. **John N. Quinton:** conceptualization, investigation, funding acquisition, writing – original draft, methodology, writing – review and editing, resources, supervision.

Acknowledgements

We would like to acknowledge UKRI grant numbers BB/Y514238/1 and NE/T012307/1. We acknowledge Mr. James Turner and Mr. Henry Scholefield for allowing us to sample the soils on their farms and Jihane Ait Bella for assisting with sensor fabrication.

Funding

This work was supported by Natural Environment Research Council and Biotechnology and Biological Sciences Research Council.

Conflicts of Interest

The authors declare no conflicts of interest.

Data Availability Statement

Data analysis, etc., is on the R Markdown site here: <https://rpubs.com/TaylorSharpe/PolyDecomp>.

References

Anthony, T. L., and W. L. Silver. 2021. “Hot Moments Drive Extreme Nitrous Oxide and Methane Emissions From Agricultural Peatlands.” *Global Change Biology* 27: 5141–5153. <https://doi.org/10.1111/GCB.15802>.

Atreya, M., S. Desousa, J. B. Kauzya, et al. 2023. “A Transient Printed Soil Decomposition Sensor Based on a Biopolymer Composite Conductor.” *Advanced Science* 10: 2205785. <https://doi.org/10.1002/ADVS.202205785>.

Atreya, M., G. Marinick, C. Baumbauer, et al. 2022. “Wax Blends as Tunable Encapsulants for Soil-Degradable Electronics.” *ACS Applied Electronic Materials* 4: 4912–4920. https://doi.org/10.1021/ACSAELM.2C00833/ASSET/IMAGES/LARGE/EL2C00833_0005.JPEG.

Bagnall, D. K., E. L. Rieke, C. L. S. Morgan, D. L. Liptzin, S. B. Cappellazzi, and C. W. Honeycutt. 2023. “A Minimum Suite of Soil Health Indicators for North American Agriculture.” *Soil Security* 10: 100084. <https://doi.org/10.1016/j.soisec.2023.100084>.

Birch, H. F. 1958. “The Effect of Soil Drying on Humus Decomposition and Nitrogen Availability.” *Plant and Soil* 10: 9–31. <https://doi.org/10.1007/BF01343734/METRICS>.

Broadbent, A. A. D., M. Bahn, W. J. Pritchard, et al. 2022. “Shrub Expansion Modulates Belowground Impacts of Changing Snow Conditions in Alpine Grasslands.” *Ecology Letters* 25: 52–64. <https://doi.org/10.1111/ELE.13903>.

Brookes, P. C., A. Landman, G. Pruden, and D. Jenkinson. 1985. “Chloroform Fumigation and the Release of Soil Nitrogen: A Rapid Direct Extraction Method to Measure Microbial Biomass Nitrogen in Soil.” *Soil Biology and Biochemistry* 17: 837–842.

Clarkson, M. O., C. S. Larkin, P. Swoboda, et al. 2024. “A Review of Measurement for Quantification of Carbon Dioxide Removal by Enhanced Weathering in Soil.” *Frontiers in Climate* 6: 1345224. <https://doi.org/10.3389/fclim.2024.1345224>.

Dey, S., and P. Tribedi. 2018. “Microbial Functional Diversity Plays an Important Role in the Degradation of Polyhydroxybutyrate (PHB) in Soil.” *3Biotech* 8: 171. <https://doi.org/10.1007/s13205-018-1201-7>.

Harmon, M. E., K. J. Nadelhoffer, and J. M. Blair. 1999. “Measuring Decomposition, Nutrient Turnover, and Stores in Plant Litter.” In *Standard Soil Methods for Long-Term Ecological Research*, 202–240. Oxford University Press.

Hayes, E. B., C. E. Norris, and J. P. Volpe. 2024. “A Field Assessment to Validate the Assumptions of the Tea Bag Index (TBI) as a Measure of Soil Health.” *Applied Soil Ecology* 195: 105256.

Hoffland, E., T. W. Kuyper, R. N. J. Comans, and R. E. Creamer. 2020. “Eco-Functionality of Organic Matter in Soils.” *Plant and Soil* 455: 1–22. <https://doi.org/10.1007/s11104-020-04651-9>.

Huang, X., Y. Li, H. Lin, et al. 2023. “Flooding Dominates Soil Microbial Carbon and Phosphorus Limitations in Poyang Lake Wetland, China.” *Catena* 232: 107468. <https://doi.org/10.1016/J.CATENA.2023.107468>.

Irving, D., S. Bakhshandeh, T. K. A. Tran, and A. B. McBratney. 2024. “A Cost-Effective Method for Quantifying Soil Respiration.” *Soil Security* 16: 100162. <https://doi.org/10.1016/j.soisec.2024.100162>.

Jackson, C. R., H. L. Tyler, and J. J. Millar. 2013. “Determination of Microbial Extracellular Enzyme Activity in Waters, Soils, and Sediments Using High Throughput Microplate Assays.” *Journal of Visualized Experiments* 80: e50399. <https://doi.org/10.3791/50399>.

Joergensen, R. G. 1996. “The Fumigation-Extraction Method to Estimate Soil Microbial Biomass: Calibration of the kEC Value.” *Soil Biology and Biochemistry* 28: 25–31. [https://doi.org/10.1016/0038-0717\(95\)00102-6](https://doi.org/10.1016/0038-0717(95)00102-6).

Joshi Gyawali, A., B. J. Lester, and R. D. Stewart. 2019. “Talking SMAAC: A New Tool to Measure Soil Respiration and Microbial Activity.” *Frontiers in Earth Science* 7: 138. <https://doi.org/10.3389/feart.2019.00138>.

Keuskamp, J. A., B. J. J. Dingemans, T. Lehtinen, J. M. Sarneel, and M. M. Hefting. 2013. “Tea Bag Index: A Novel Approach to Collect Uniform Decomposition Data Across Ecosystems.” *Methods in Ecology and Evolution* 4: 1070–1075. <https://doi.org/10.1111/2041-210X.12097>.

Lehmann, J., D. A. Bossio, I. Kögel-Knabner, and M. C. Rillig. 2020. “The Concept and Future Prospects of Soil Health.” *Nature Reviews Earth & Environment* 1: 544–553. <https://doi.org/10.1038/s43017-020-0080-8>.

Macagga, R., M. Asante, G. Sossa, D. Antonijević, M. Dubbert, and M. Hoffmann. 2024. “Validation and Field Application of a Low-Cost Device to Measure CO₂ and Evapotranspiration (ET) Fluxes.” *Atmospheric Measurement Techniques* 17: 1317–1332. <https://doi.org/10.5194/amt-17-1317-2024>.

Middleton, T. E., A. L. McCombs, S. R. Gailans, et al. 2021. “Assessing Biological Soil Health Through Decomposition of Inexpensive Household Items.” *Applied Soil Ecology* 168: 104099. <https://doi.org/10.1016/j.apsoil.2021.104099>.

Pinheiro, J. C., and D. M. Bates. 2000. *Mixed-Effects Models in S and S-PLUS*. Springer. <https://doi.org/10.1007/b98882>.

Pinheiro, J., D. Bates, and R Core Team. 2023. *NLME: Linear and Nonlinear Mixed Effects Models*. R Package Version 3. [Code]. <https://cran.r-project.org/web/packages/nlme/index.html>.

Poffenbarger, H., M. Castellano, D. Egli, A. Jaconi, and V. Moore. 2023. “Contributions of Plant Breeding to Soil Carbon Storage: Retrospect and Prospects.” *Crop Science* 63: 990–1018. <https://doi.org/10.1002/csc2.20920>.

R Core Team. 2025. *R: A Language and Environment for Statistical Computing*. R Foundation for Statistical Computing [Code]. <https://posit.co/download/rstudio-desktop>.

Regina, K., and L. Alakukku. 2010. “Greenhouse Gas Fluxes in Varying Soils Types Under Conventional and No-Tillage Practices.” *Soil and*

Tillage Research 109: 144–152. <https://doi.org/10.1016/J.STILL.2010.05.009>.

Ryan, M. G., and B. E. Law. 2005. “Interpreting, Measuring, and Modeling Soil Respiration.” *Biogeochemistry* 73: 3–27. <https://doi.org/10.1007/S10533-004-5167-7/METRICS>.

Sánchez-Rodríguez, A. R., P. W. Hill, D. R. Chadwick, and D. L. Jones. 2019. “Typology of Extreme Flood Event Leads to Differential Impacts on Soil Functioning.” *Soil Biology & Biochemistry* 129: 153–168. <https://doi.org/10.1016/J.SOILBIO.2018.11.019>.

Sharpe, T. J., M. Atreya, S. Liu, et al. 2026. “In-Situ Decomposition Sensor Output Correlates With Soil Health Indicators.” *Computers and Electronics in Agriculture* 244: 111427. <https://doi.org/10.1016/j.compag.2026.111427>.

Singh, S., M. A. Mayes, S. N. Kivlin, and S. Jagadamma. 2023. “How the Birch Effect Differs in Mechanisms and Magnitudes due to Soil Texture.” *Soil Biology & Biochemistry* 179: 108973. <https://doi.org/10.1016/J.SOILBIO.2023.108973>.

Sinsabaugh, R. L. 2010. “Phenol Oxidase, Peroxidase and Organic Matter Dynamics of Soil.” *Soil Biology and Biochemistry* 42: 391–404. <https://doi.org/10.1016/j.soilbio.2009.10.014>.

Tate, R. L., III. 1979. “Effect of Flooding on Microbial Activities in Organic Soils: Carbon Metabolism.” *Soil Science* 128: 267–273.

Yamauchi, T., S. Shimamura, M. Nakazono, and T. Mochizuki. 2013. “Aerenchyma Formation in Crop Species: A Review.” *Field Crops Research* 152: 8–16.

Zeng, X., X. Chen, L. Heng, S. O. Oshunsanya, and H. Yu. 2026. “Application of a High-Performance, Low-Cost Portable NDIR Sensor Monitoring System for Continuous Measurements of In Situ Soil CO₂ Fluxes.” *Sensors* 26: 761.

Supporting Information

Additional supporting information can be found online in the Supporting Information section. **Table S1:** Two-way ANOVA results of treatment effects on soil parameters at harvest.